Ionics (2019) 25:1177–1185
https://doi.org/10.1007/s11581-018-2778-x

ORIGINAL PAPER

Preparation and application of malachite green molecularly imprinted/gold nanoparticle composite film–modified glassy carbon electrode

Yaqing Xu[1,2] · **Zhiyue Gao**[3] · **Wen Chen**[1,2] · **Er Wang**[4] · **Yan Li**[1,2]

Received: 16 August 2018 / Revised: 2 October 2018 / Accepted: 27 October 2018 / Published online: 28 November 2018

Abstract

A kind of new malachite green (MG) polypyrrole (PPy) molecularly imprinted (MIP)/gold nanoparticle composite (AuNPs) film–modified glassy carbon electrode (MG-MIPPPy/AuNPs/GCE) was prepared by potentiostatic deposition of gold nanoparticle on glassy carbon electrode at − 0.2 V (vs. SCE) for 100 s, pyrrole (Py) as monomer, and MG as template molecule (molar ratio = 1:1) by cyclic voltammetry (CV) electropolymerization. And various modified electrodes were characterized by SEM and EIS and CV methods. Potassium ferricyanide was used as a probe; the concentration of MG was indirectly detected by the linear relationship between the current change value (ΔI_{DPV}) and the logarithm value of concentration of MG. Under the optimal conditions, there was a linear relationship between the ΔI_{DPV} and the negative logarithm of concentration in the range of 2.73×10^{-9} M ~ 2.74×10^{-6} M ($R = 0.9961$). The detection limit is 3.57×10^{-11} M ($S/N = 3$). The sample recovery was 98.82 to 103.38%. These analysis results of real samples were satisfactory.

Keywords Molecularly imprinted polymer · Gold nanoparticles · Malachite green · Glassy carbon electrode

Introduction

Malachite green (MG) is a toxic triphenylmethane organic compound that is both dye, bactericidal, and parasite chemical agent. In recent years, it was found that malachite green compounds and their metabolites are highly residual, toxic, and produce carcinogenic, teratogenic, mutagenic, and other side effects [1]. The scientific studies have shown that the longer the residual time in fish and aquatic animals, the more likely it is to cause malformation or even cancer [2]. At the same time, it will bring potential risks for consumers when they eat the products with residues of MG. So, it has been listed as the banned drugs in aquaculture in many countries. As early as May 2002, MG was included in the list of banned veterinary drugs and compounds for edible animals in our country. However, MG has special effects on saprolegniaceae disease of fish and its eggs and there is no specific drug that can cure saprolegniaceae disease in the market for a short time, which is the fundamental reason why malachite green has been repeatedly banned in the aquaculture industry, but there are still many cases of illegal use. It seriously affected the competitiveness and reputation in the international market of Chinese aquatic products. For health reasons, and supervision of the quality of aquatic products, it is very important to establish a fast and simple method for the determination of MG in aqueous samples.

The traditional techniques of MG detection mainly include high-performance liquid chromatography (HPLC) [3–5], spectrophotometry [6, 7], and enzyme-linked immunosorbent assay (ELISA) [8, 9]. For routine analyses, these methods are

---

Wen Chen and Er Wang contributed equally to this work.

✉ Wen Chen
chenwen2010@foxmail.com

✉ Er Wang
scwanger@foxmail.com

[1] College of Materials and Chemistry & Chemical Engineering, Chengdu University of Technology, Chengdu 610059, Sichuan, People's Republic of China

[2] Mineral Resources Chemistry Key Laboratory of Sichuan Higher Education Institution, Chengdu 610059, Sichuan, People's Republic of China

[3] Sichuan Provincial Chuanjian Institute of Investigation and Design, Chengdu 610015, Sichuan, People's Republic of China

[4] Analysis Laboratory 280 Research Institute of Nuclear Industry, Guanghan 618300, Sichuan, People's Republic of China

reliable and sensitive, but several disadvantages need to be solved, such as the high cost, the need of well-trained operators, the complex sample preparation, and the impossibility to be moved to on-site detection in case of an emergent pollution incident.

Electrochemical methods [10–14] have been found to be highly sensitive, convenient, with on-site possible detection, and effective tool for the analysis [15–17]. However, in general, bare electrodes have the problems of low sensitivity, narrow detection range, and poor selectivity, which need to be improved by modification of electrode surface. Alireza Nezamzadeh-Ejhieh et al. have done a lot of research on modified electrode [18–20]; the importance of electrode modification has been proved. Without electrode modification, there is no sensor with high sensitivity and selectivity. Such as the graphene quantum dots and gold nanoparticle–modified glassy carbon electrode (GR-QDS/AuNP/GCE) [11], Au nanoparticle-chitosan/multi-walled carbon nanotube–modified glassy carbon electrode (AuNP-CS/MWNT/GCE) [12], CeO_2/Nafion/GCE [13], and MWNT-DHP (dihexadecyl hydrogen phosphate)/GCE [14] were used to detect MG (as shown in Table 1). These modified electrodes have either a low detection limit or a wide detection range. But most of them cannot be reused and need to be modified repeatedly, which is also a difficult problem for the most of composite film–modified electrode to be solved.

Electrochemical sensors based on molecularly imprinted polymer (MIP) not only have the good sensitivity and wide detection range, but also can be used repeatedly. To a certain extent, it solves the problem that the composite film–modified electrode cannot be reused. And the determination of MG by molecularly imprinted sensors has not been reported at present.

However, only the MIP film is used as the sensor identification element; usually, there are disadvantages of poor adsorption capacity and low sensitivity. In order to achieve the excellent performance of the molecular imprinting sensor, it is necessary to amplify the current signal, shorten the response time, and completely remove the template molecule and so on [16].

It is reported that gold nanoparticles have excellent electrocatalytic properties; they are biocompatible with other advantages and have been widely used in molecular imprinting electrochemical sensor performance improvement [21–24]. For example, G. C. Zhao et al. [25] improved the electrochemical signal by 2.6 times after modifying gold nanoparticles with molecularly imprinted electrodes, because the AuNPs were modified on the base electrode and constructed the composite film–modified electrode with MIP. The gold nanoparticles can increase the surface area and recognition unit of the modified electrode, increase the conductivity and electron transport capability of the MIP film, and finally, significantly improve the sensitivity of the molecularly imprinted modified electrode [26]. Therefore, the preparation and application of MG-MIPPy/AuNPs/GCE has been studied in this work.

Preparation of MG-MIPPy/AuNP composite electrochemical sensor was studied in this work. And considering the lower sensitivity of direct response of MG on the composite film of MG-MIPPy/AuNPs/GCE, the potassium ferricyanide ($K_3Fe(CN)_6$) was selected as the probe to detect MG indirectly according to the reported literature [27]. It is based on the selective occupation of MG on the adsorption site of MG-MIPPy/AuNPs/GCE, preventing the probe molecules from entering and reducing its peak current. In most modified electrodes, peak current tend to increase in presence of analyte, rarely it decreased, while the decrease of current change was applied in this study to detect MG indirectly, so as Motahare Nosuhi et al. did [28].

There was a linear relationship between the changes of current value (ΔI_{DPV}) and the logarithm value of concentration of MG. Then, a new electrochemical analysis method for determination of MG indirectly was established. The sensor showed high sensitivity, good reproducibility, and stability. Furthermore, this method was successfully applied to detect MG in fish pond water, river, and lake with satisfactory recoveries.

Experimental

Reagents and materials

Malachite green was purchased from Tianjin Tianda Chemical Co., Ltd. Pyrrole (99%) was provided by Shanghai Lirui Biological Technology Co., Ltd. $K_3Fe(CN)_6$, $HAuCl_4 \cdot 4H_2O$ (Au% > 47%), $Na_2HPO_4 \cdot 12H_2O$, $NaH_2PO_4 \cdot 2H_2O$, H_2SO_4, and KCl were obtained from Chengdu Kelong Chemical Reagent Co., Ltd. Ultrapure water (Milli-Q water with 18.2 MΩ cm) used throughout the study and others were analytical grade reagents.

Instrument

An Autolab PGSTAT 302N (Metrohm-Autolab, Metrohm Co., Ltd., China) was used for electrochemical studies connected to a conventional three-electrode system [29]. A saturated calomel electrode (SCE) was used as the reference electrode, while a platinum electrode was the auxiliary electrode, and a GCE (3 mm in diameter, Tianjin Aida, China) or a GCE modified by different methods was used as working electrodes. Nova Nano SEM450/FEI (USA) were used to obtain the scanning electron microscope (SEM) images.

Table 1 Comparison of MG determination with different modified electrodes

Modified electrodes	Linear range (M)	Detection limit (M)
GR-QDS/AuNPs/GCE [11]	4.00×10^{-7} to 1.00×10^{-5}	1.00×10^{-7}
AuNPs-CS//MWNTsGCE [12]	2.50×10^{-9} to 2.50×10^{-4}	9.30×10^{-10}
CeO_2/Nafion/GCE [13]	1.00×10^{-6} to 8.00×10^{-5}	1.00×10^{-6}
MWNT-DHP/GCE [14]	5.00×10^{-8} to 8.00×10^{-6}	6.00×10^{-9}
This work	2.74×10^{-9} to 2.74×10^{-6}	3.57×10^{-11}

Au NPs Au nanoparticles, *CS* chitosan, *MWNTs* multi-walled carbon nanotubes, *GR-QDS* graphene quantum dots, *DHP* dihexadecyl hydrogen phosphate

Senor fabrication

The procedure to obtain the imprinted sensor is illustrated in Scheme 1. Firstly, a bare GCE was polished with an alumina slurry of 0.5 μm and then 0.3 μm α-Al_2O_3 particles on a polishing cloth, and was sequentially sonicated in ethanol and ultrapure water for 3 min. The electrode was then activated in 0.5 M H_2SO_4 by cycling the potential between − 0.2 and + 0.8 V at a 100 mV/s scanning rate until stable CV was obtained. The electrode was rinsed with ultrapure water and dried under nitrogen at last. All measurements were at room temperature.

The pretreated GCE was immersed into a 10-mL small beaker of 10 mM $HAuCl_4$ containing 0.1 M Na_2SO_4 solution and subjected to a negative potential by applying − 0.2 V (vs. SCE) for 100 s, leading AuNPs electrodeposited onto the surface of the GCE. It was then washed with ultrapure water and blown with nitrogen [30].

The polypyrrole film with MG imprinting/AuNPs/GCE was obtained using cyclic voltammetry scanning in the potential range from − 0.2 to + 1.0 V (vs. SCE) at 50 mV s^{-1} during 20 cycles in the solution containing 0.05 M pyrrole, 0.05 M MG, and 0.1 M KCl with 0.5 M phosphate buffer solution (PBS, pH = 6.9). After that, the electrode was over oxidized at the constant potential of 1.3 V (vs. SCE) by chronoamperometry for 5 min in a 0.2 M Na_2HPO_4 solution, and then ultrasonically cleaned in ultrapure water for 3 min to remove template molecules adequately. At last, MG-MIPPy/AuNPs/GCE were washed with ultrapure water and further used after drying under nitrogen. Non-imprinted polymer (NIP) electrode was prepared under the same experimental conditions but without MG in the solution.

Electrochemical measurements

The electrochemical behavior of the molecularly imprinted films were studied by CV in a 0.1 M KCl solution containing 5 mM $K_3[Fe(CN)_6]$. The DPV measurements were performed with $K_3[Fe\ (CN)_6]$ and MG-MIPPy/AuNPs/GCE at potential from − 0.2 to − 0.6 V, at the scanning rate of 50 mV/s, with a pulse amplitude of 50 mV and a pulse width of 50 ms, after a 10 min incubation time in the containing MG. The MG was indirectly detected by measuring the changes value of peak current (ΔI_{DPV}) of the $K_3\ [Fe(CN)_6]$ probe.

Real sample collection

The polyethylene plastic sampling bottle was soaked with HNO_3 (10%) for 3 days and washed with ultrapure water. The four sampling points (Dongfeng canal, Yan Lake, and two fish ponds) were selected, and the bottles were washed with water samples for 3~5 times, taking water samples at about 0.5 and 1 m depth, and then mix each other. 50 mL water sample was taken in 100 mL beaker, respectively,

Scheme 1 Scheme of preparation and regeneration process of MG-MIPPy/AuNPs/GCE

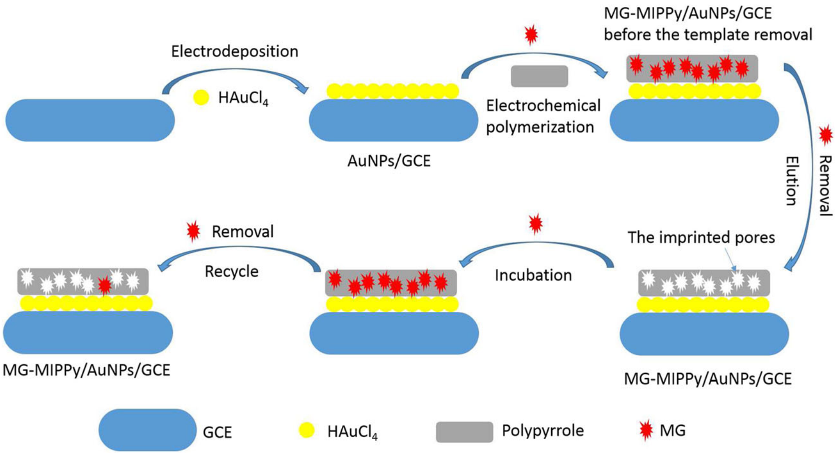

added about 2 mL 0.02 mol/L NaOH solution, then centrifuged, and 5.0 mL of the supernatant was used to adjust pH to about 7 with HCl solution of 0.02 mol/L, and then pH = 6.9 PBS buffer solution was used to dissolve in 10-mL colorimetric tube, respectively. The measurement and the recovery test of the sample solution were carried out according to the experimental method.

Results and discussion

Preparation of MG-MIPPy/AuNP composite electrode

The process of electropolymerization of MG-MIPPy and NIP films by the CV is shown in Fig. 1. The obvious oxidation peak appears at 0.65 V (vs. SCE) in the first scan of electropolymerization of MG-MIP (Fig. 1a), while there is no any peak during electropolymerization of NIP (Fig. 1b). This may be due to the reason that MG can catalyze the electrochemical oxidation of pyrrole. Figure 1a shows the amplitude decreases sharply as long as the potential cycling continues; moreover, there is no reduction wave in any cycle. It indicates the MG-MIPPy thin film was successfully formed on the GCE mainly in the first half-cycle, which blocks the electrode surface; the electrochemical process of pyrrole was completely irreversible, and the anodic peak only appeared in the first cycle, at about 0.65 V (vs. SCE) [31].

These results are consistent with the sequence of reactions, including the oxidation of –NH– of pyrrole monomers, polymerization, and the deposition of stable MG coatings on the surface of AuNPs/GCE. The MG template molecules are embedded in the polymer matrix by electrodeposition of the conductive polymer, and after the peroxidation treatment, the polymer film loses conductivity and the imprint holes of MG were left after eluting the template molecules. The N in the MG template molecule is able to bond together with the –NH– on the imprinted hole in the form of hydrogen bonds.

SEM morphology of the electrode

The morphology of AuNPs/GCE and MG-MIPPy/AuNP/GCE surfaces was characterized by SEM. Figure 2a shows the smooth surface of the AuNPs/GCE, and many AuNPs with a diameter of ca. 10 nm deposited on the surface of GCE in the shape of metallic clusters. But, when the MG-MIPPy was further polymerized on AuNP/GCE surface by cyclic voltammetry, the AuNPs were evenly distributed in its membrane; obviously, the imprinted film of MG-MIPPy/AuNPs/GCE became rough after removal, shown in Fig. 2b.

Electrochemical characteristics of the modified electrode

Electrochemical impedance spectroscopy (EIS) was obtained in the solution of 5.0 mM $Fe(CN)_6^{3-/4-}$ containing 0.1 M KCl by setting frequency range from 10^{-2} to 10^5 Hz and the potential to 0.2 V [30]. To study the effect of calcination temperature onto the charge transfer ability of the modified electrodes with modifier, the corresponding Nyquist plots are shown in Fig. 3. The Nyquist curve's high frequency semicircle part is related to the electron transfer process [15, 29]. As shown in Fig. 3, the curve semicircle radius of the bare electrode is larger than that of modified by AuNPs. It is proved that gold nanoparticle can enhance the conductivity of the electrode. The electron transfer resistance of MG-MIPPy film increased sharply after deposited on AuNPs/GCE by CV; the electron conductivity was reduced due to the formation of the MG-MIPPy. It made $[Fe(CN)_6]^{3-/4-}$ unable to reach the electrode surface because of the good insulation properties of the MG-MIPPy film. After the MG template molecule was removed, there were imprinted holes in the MIP film, which makes it easier for $K_3[Fe(CN)_6]$ to transfer to the electrode surface; it led to the decrease of EIS immediately, which further proves the existence of the molecularly imprinted hole on the composite film of the modified electrode [32]. The holes identified as imprinted holes of malachite green have been demonstrated by interference experiments (Table 2). The corresponding Bodes' plots were obtained by data fitting using "Nova" software. The corresponding equivalent electrochemical circuit is shown in inset of Fig. 3. As shown, the circuit includes three resistances (solution, Rs, polarization, Rp or Rct, and charging resistances from left to right, respectively) and one capacitor. One of the capacitors has parallel plans; it should be considered as a non-ideal capacitor or constant phase element (CPE)

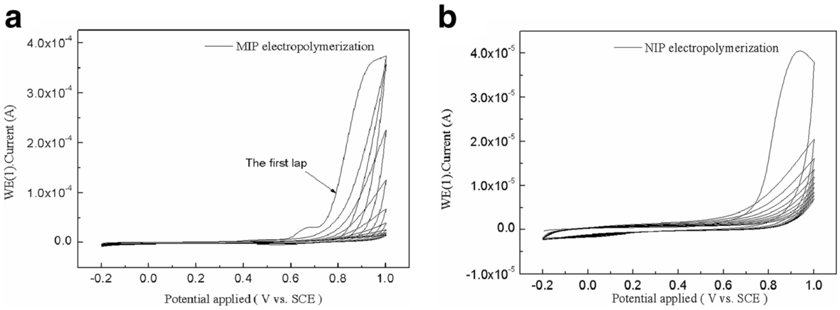

Fig. 1 The cyclic voltammetry curve of the electropolymerization process [in the solution containing 0.05 M pyrrole, 0.05 M MG, and 0.1 M KCl with 0.5 M phosphate buffer solution (PBS, pH = 6.9)]. **a** MG-MIPPy/AuNPs/GCE. **b** NIPPy/AuNPs/GCE

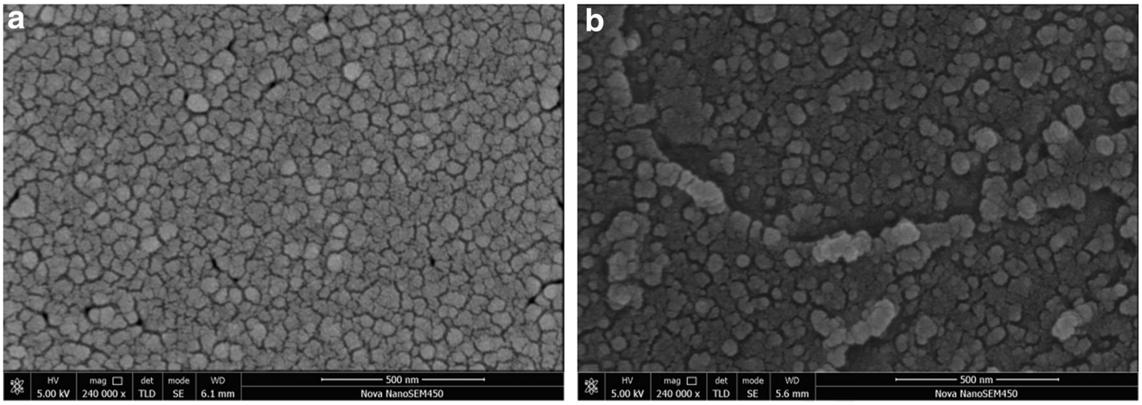

Fig. 2 SEM images of AuNPs/GCE (**a**) and MIPPy/AuNPs/GCE (**b**)

[33]. The R_{ct} value of each electrode is fitted from the equivalent circuit in Fig. 3. The equivalent circuit R_{ct} value of the modified electrodes was as follows: MG-MIPPy/AuNPs/GCE before the template removal (45.3 kΩ) > MG-MIPPy/AuNPs/GCE after the template removal (869 Ω) > GCE (168 Ω) > AuNPs/GCE (85 Ω). On the other hand, the result proved that the modified electrode was prepared successfully.

The cyclic voltammograms of the modified electrodes in 5 mM $K_3[Fe(CN)_6]$ (Fig. 4) could further evidenced the electrochemical characteristics of the modified electrode [15]. The oxidation and reduction peak current of the modified MIPPy/AuNPs/GCE after the template removal (curve 3) was higher than the current of the MIPPy/GCE after the template removal (curve 4), while the AuNPs/GCE (curve 1) is higher than the bare GCE electrode (curve 2). Therefore, the AuNP–modified electrode can increase the contact area between the electroactive material and the electrode surface, and generate more transmission channels to promote the diffusion and the redox reaction $[Fe(CN)_6]^{3-/4-}$ on the electrode surface. The redox peak of the NIP (curve 6) and MG-MIP (curve 5) was hardly observed after the polymerization of the pyrrole, because the MG-MIPPy film is covering the surface of the electrode and blocked the conduction of the electrons. The redox peaks were observed again when the MG template was removed (curve 3), whereas NIPPy did not show significant redox peaks due to the lack of template molecules. It was then proved that MG-MIPPy was formed successfully.

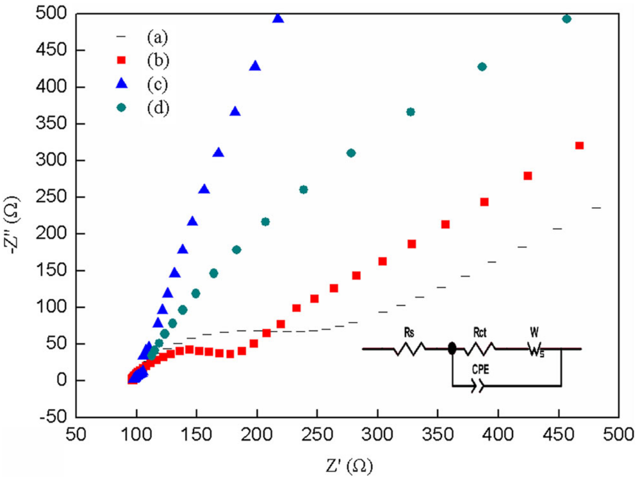

Fig. 3 Electrochemical impendence spectroscopy (EIS) of GCE (a), AuNPs/GCE (b), MG-MIPPy/AuNPs/GCE before the template removal (c), and MG-MIPPy/AuNPs/GCE after the template removal (d) (in the solution of 5.0 mM $Fe(CN)_6^{3-/4-}$ containing 0.1 M KCl by setting frequency range from 10^{-2} to 10^5 Hz and the potential to 0.2 V)

Optimization of the experimental conditions

Buffer and the ratio of the monomer to template

The peak current in different buffer solutions was evaluated for electropolymerization conditions [34]. It was found that PBS performed best in B-R buffer, PBS buffer, sodium citrate buffer, and NaAc-HAc buffer. The proper proportion of monomer and template molecules has a very important effect on the specificity and selectivity of molecularly imprinted film [35]. When the ratio of the monomer to the template (monomer/template) is small, excessive template will prevent the pyrrole monomer from binding to MG to form an effective adsorption site.

On the contrary, when the amount of monomer is too large, it is easy to polymerize directly between the monomers, making it difficult to form more effective imprinting sites. From Fig. 5a, when the ratio of the monomer to MG template is 1:1, the current change (ΔI_{DPV}) before and after MG template elution is the largest [36]. So, the ratio of the monomer to MG template 1:1 was chosen.

The polymerization cycles

At the same time, the thickness of the MG-MIPPy film also affects the electron transfer; the thickness of the polymer film can be controlled by the number of polymerization cycles. The effect of numbers of cycles was studied from 12 to 32 on ΔI_{DPV}. As shown in Fig. 5b, ΔI_{DPV} increases with the cycle number from 12 to 20, and

Table 2 Influences of possible interferences for MG (2.74×10^{-7} M)

Interferences	Concentration of interference (10^{-7} M)	Signal change (%)	Interferences	Concentration of interference (10^{-7} M)	Signal change (%)
Na^+	411	+ 4.33	Pb^{2+}	137	+ 4.89
K^+	411	+ 4.23	Cl^-	548	− 5.12
Fe^{3+}	164	+ 5.08	CO_3^{2-}	548	− 5.05
Mg^{2+}	137	+ 4.56.	NO_3^-	548	− 5.44
Ca^{2+}	137	+ 4.77	SO_4^{2-}	548	− 5.04
Cu^{2+}	548	+ 4.56	Crystal violet	548	+ 4.85
Ni^{2+}	411	+ 4.98	Phenolphthalein	411	+ 4.94

reached a maximum value at 20 cycles. As the number of cycles increases until 32, ΔI_{DPV} gradually decreased. Therefore, 20 CV cycles were chosen to prepare the polymer film in optimal condition.

Elution condition

To obtain satisfactory sensitivity and selectivity, it is very important to elute the MG template from MIP film completely. In our work, different solvents to remove the template from MG-MIPPy/AuNPs/GCE were studied, such as water, NaOH, ethanol, and NaH_2PO_4. The most efficient removal solvent was found to be 0.2 M NaH_2PO_4 with an ultrasonic cleaning for 3 min to completely elute the template. As shown in Fig. 5c, the elution time on the MG-MIPPy film also has a great impact on the firmness. When the peroxide time is too short, the MG template molecules cannot be removed effectively; on the other hand, if the time is too long, it will lead to the film off and reduce the possibility for the modified electrode to be re-used. Therefore, the elution time was set to 300 s.

Incubation condition

As shown in Fig. 5d, the effect of the incubation time ranging from 2 to 16 min on ΔI_{DPV} was investigated. As the incubation time increased, the current increased rapidly until 10 min to reach a constant value, related to the adsorption equilibrium. Therefore, 10 min was chosen as the appropriate incubation time.

Linear range and limit of detection

Under optimized conditions, the ΔI_{DPV} response of the electrode in 0.1 M KCl containing 5 mM $K_3[Fe(CN)_6]$ solutions after incubation in PBS (pH = 6.9): MG (V:V = 1:1) was shown in Fig. 6. It can be seen that ΔI_{DPV} decreases gradually with the increase of MG concentration [15]. There was a linear relationship between negative logarithm values of MG concentrations varying from 2.74×10^{-9} M to 2.74×10^{-6} M (Fig. 6). The linear regression equation is $\Delta I(\mu A) = 5.1143 \log C + 15.398$ ($R = 0.9961$). The detection limit was estimated to be 3.57×10^{-11} M ($S/N = 3$), indicating that the MG-MIPPy/AuNPs/GCE had a fairer sensitivity, a wider linear range, and

Fig. 4 Cyclic voltammograms of different electrodes recorded in 5 mM $K_3[Fe(CN)_6]$containing 0.1 M KCl, (1) AuNPs/GCE, (2) GCE, (3) MG-MIPPy/AuNPs/GCE after the template removal, (4) MG-MIPPy/GCE after the template removal, (5) MG-MIPPy/AuNPs/GCE before the template removal, (6) NIPPy/AuNPs/GCE

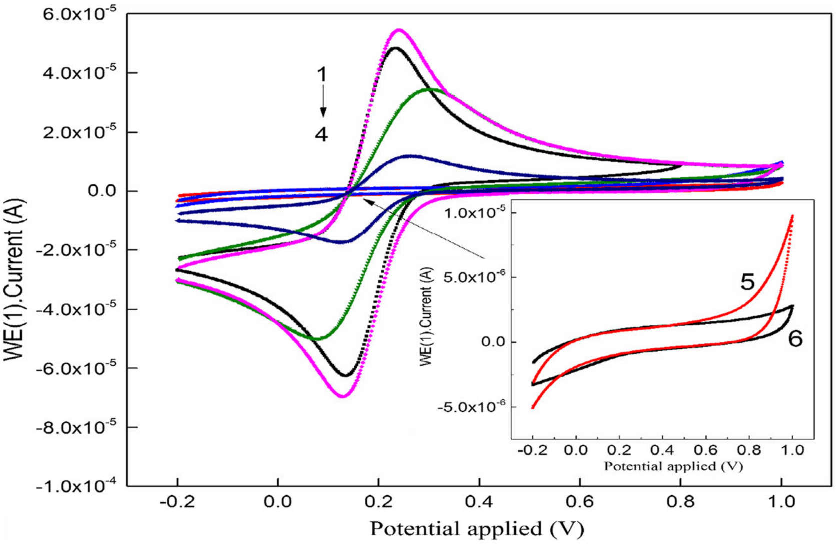

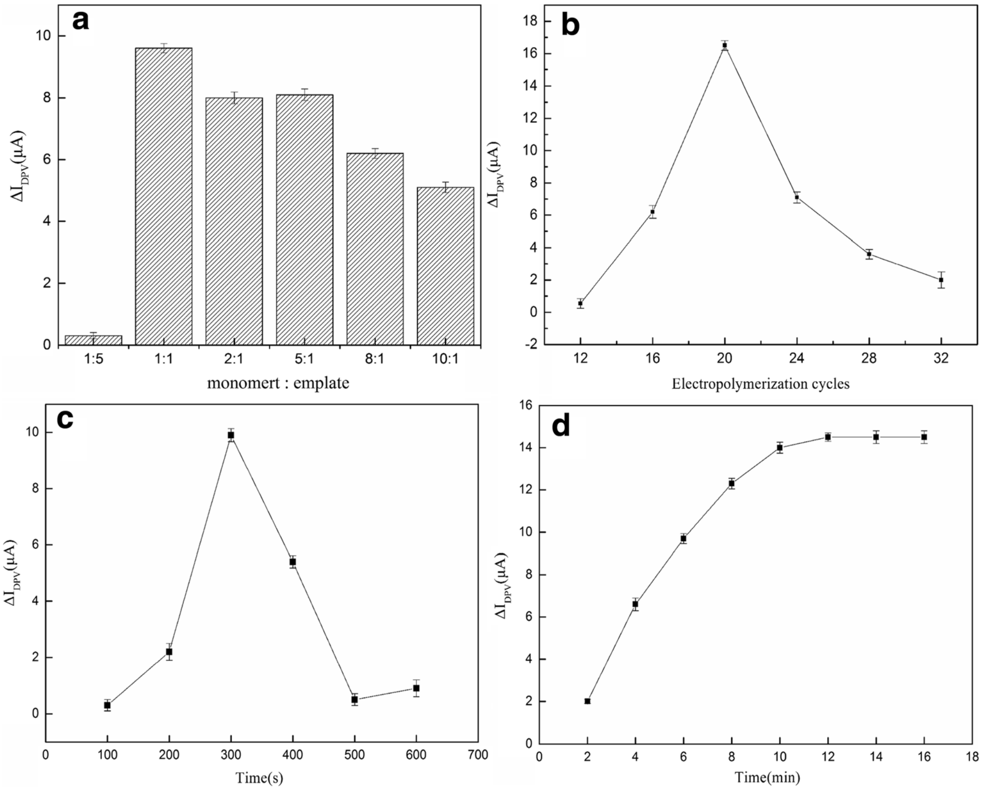

Fig. 5 Optimization of the experimental conditions about the current changes (ΔI_{DPV}) at MIPPy/AuNPs/GCE **a** monomer to template ratio, **b** electropolymerization cycle, **c** elution time, and **d** incubation time

a lower detection limit. Compared with those of other reported electrochemical sensors, the detection range is wider and the detection limit is lower for MG determination [30] (Table 1).

Reproducibility, stability, and selectivity

The relative standard deviation (RSD) was 3.71% with 4 repeated measurements on a single electrode. By comparing the responses of three similar independent electrodes, the variation between electrodes was studied by statistical g-test. Comparison of $g_{exp} = 1$ with $g_{0.05,4,3} = 1.135$. The results show that the electrode has good reproducibility in the confidence interval of 0.95% [37].

The electrode's metrological parameters did not significantly deteriorate at least after 16 numbers of samples were determined.

For the investigation of the stability of the senor, the electrode was stored at 4 °C after determined of ΔI_{DPV}. Two weeks later, the current response represents 96.3% of the initial peak

Fig. 6 The current of DPV for the different concentrations of MG at MIP/AuNP/GCE–modified electrode. (a) 2.74×10^{-9} M. (b) 2.74×10^{-8} M. (c) 8.22×10^{-8} M. (d) 2.74×10^{-7} M. (e) 5.48×10^{-7} M. (f) 1.37×10^{-6} M. (g) 1.92×10^{-6} M. (h) 2.74×10^{-6} M

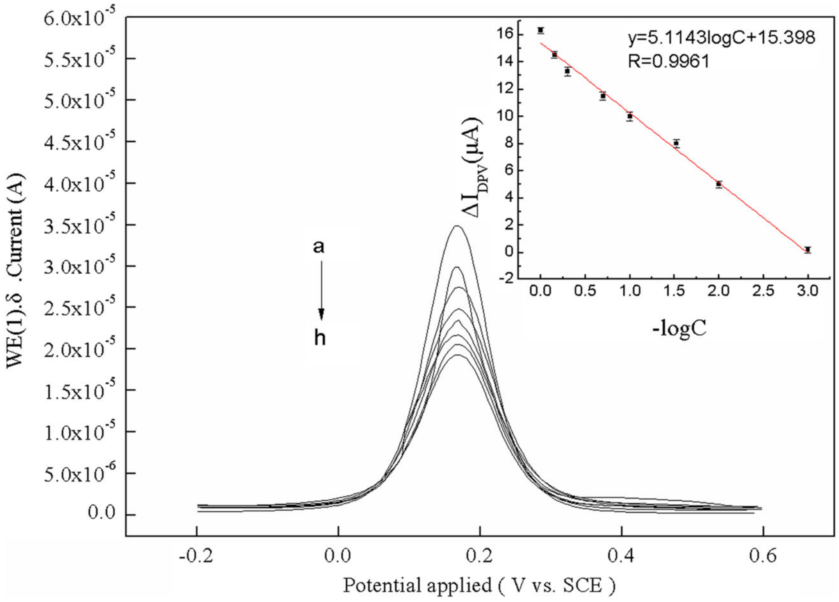

Table 3 Determination of MG in aqueous environmental samples

Sample	Original average ($N = 3.10^{-9}$ M)	Added MG (10^{-9} M)	RSD (%)	Recovery (%)
1st fish pond	8.29	8.22	0.53	102.00
				100.07
				100.23
2nd fish pond	11.07	10.96	0.72	101.68
				99.72
				98.82
Yan Lake	ND	13.70	1.61	99.85
				101.06
				103.08
Dongfeng canal	ND	13.70	1.19	101.10
				101.08
				99.02

ND not detected

current. This showed that the imprinted sensor had a long-term stability [29].

The interference resistance of the sensor was investigated through experiments of coexisting substances. The effects of crystal violet, phenolphthalein, common anions, and cationic added in the water were investigated. As listed in Table 2, among them, Mg^{2+}, Ca^{2+}, and Pb^{2+} have slight interference; this interference can be eliminated by precipitation separation or complex masking, and other substances have no interfere at all. Especially, crystal violet and phenolphthalein belong to triphenylmethane dyes which have similar structure to malachite green, but there is no interference when their concentration is much greater than that of malachite (548×10^{-7} M and 411×10^{-7} M respectively), which further proves the existence of molecular imprinting of malachite green. Thus, a good selectivity can be achieved with this sensor.

Analysis of real water samples

The feasibility of the modified electrode was evaluated by analyzing real water samples. The samples were collected according to the experimental methods and then added 2 mL 0.02 M NaOH to separate interference ions. Then, the pH was adjusted to 7.

The results showed that the recovery was from 98.82 to 103.38%. It has been proved that MG-MIPPy/AuNPs/GCE is reliable and efficient for the detection of MG in real samples (Table 3).

Conclusions

In this work, the results confirmed that AuNPs could increase the conductivity of the sensor and significantly increase the response current. The MG-MIPPy/AuNP composite electrode has a specific three-dimensional imprinted cavities with recognition site of the MG; it will be occupied selectively when MG is present in the sample, which prevents the probe molecules from entering the surface of electrode and resulted in the decrease of the peak currents in $K_3[Fe(CN)_6]$ redox probe [15, 28]. This new method exhibits good selectivity, high sensitivity, and good stability over time.

References

1. Culp SJ, Mellick PW, Trorrer RW (2006) Carcinogenicity of malachite green chloride and leucomalachite green in B6C3F1 mice and F344 rats. Food Chem Toxicol 44:1204–1212
2. Program NT (2005) Toxicology and carcinogenesis studies of malachite green chloride and leucomalachite green. (CAS NOS. 569–64-2 and 129–73-7) in F344/N rats and B6C3F1 mice (feed studies). Natl Toxicol Program Tech Rep 527:1–312
3. Wang LL, Feng XP, Hu EP (2007) Survey of malachite green residues in aquatic foods and pool water from restaurant in Zhuhai. Chin J Health Lab Technol 17:1687–1689
4. Hernando MD, Mezcua M, Suárez-Barcena JM (2006) Liquid chromatography with time-of-flight mass spectrometry for simultaneous determination of chemotherapeutant residues in salmon. Anal Chim Acta 562:176–178
5. Chen G, Miao S (2010) HPLC determination and MS confirmation of malachite green, gentian violet, and their leuco metabolite residues in channel catfish muscle. J Agric Food Chem 58:7109–7114
6. Sadi A, Leonardi LS, Cury J (2014) Graphene oxide magnetic nanocomposites for the preconcentration of trace amounts of malachite green from fish and water samples prior to determination by fiber optic-linear array detection spectrophotometry. Anal Methods 6:7744–7751
7. Liu LJ (2011) Time-Offset Compensation Based Time Synchronization Approach for Wireless Sensor Network. Chin J Spectrosc Lab 28:41–46

8. Xing W, He L, Yang H, Sun C, Li D, Yang X, Li Y, Deng A (2009) Development of a sensitive and group-specific polyclonal antibody-based enzyme-linked immunosorbent assay (ELISA) for detection of malachite green and leucomalachite green in water and fish samples. J Sci Food Agric 89:2165–2173
9. Wang F, Wang H, Shen Y et al (2016) Bispecific Monoclonal Antibody-Based Multianalyte ELISA for Furaltadone Metabolite, Malachite Green, and Leucomalachite Green in Aquatic Products. J Agric Food Chem 64:8054–8061
10. Zhu D, Li QQ, Pan XM et al (2016) A sensitive electrochemical impedance immunosensor for determination of malachite green and leucomalachite green in the aqueous environment. Anal Bioanal Chem 408:5593–5600
11. Hou J, Bei F, Wang M, Ai S (2013) Electrochemical determination of malachite green at graphene quantum dots–gold nanoparticles multilayers–modified glassy carbon electrode. J Appl Electrochem 43:689–696
12. Liu YY, Ning BA, Bai JL, et al. (2014) AuNPs-chitosan/MWNTs modified GCE used for detection of trace malachite green in water. J Food Saf Qual 5:1468–1474
13. Sacara AM, Cristea C, Muresan LM (2017) Electrochemical detection of Malachite Green using glassy carbon electrodes modified with CeO 2 nanoparticles and Nafion. J Electroanal Chem 792:23–30
14. Yi H, Qu W, Huang W (2008) Electrochemical determination of malachite green using a multi-wall carbon nanotube modified glassy carbon electrode. Microchimica Acta 160(1-2): 291–296
15. Tan F, Cong LC, Li XN et al (2016) An electrochemical sensor based on molecularly imprinted polypyrrole/graphene quantum dots composite for detection of bisphenol A in water samples. Sensors Actuators B Chem 233:599–606
16. Silva Hd, Pacheco J, Silva J (2015) Molecularly imprinted sensor for voltammetric detection of norfloxacin. Sensors Actuators B Chem 219:301–307
17. Sharafzadeh S, Nezamzadeh-Ejhieh A (2015) Using of anionic adsorption property of a surfactant modified clinoptilolite nanoparticles in modification of carbon paste electrode as effective ingredient for determination of anionic ascorbic acid species in presence of cationic dopamine species. Electrochim Acta 184:371–380
18. Mahdavi M, Nezamzadeh-Ejhieh A (2017) An aluminum selective electrode via modification of PVC membrane by modified clinoptilolite nanoparticles with hexadecyltrimethyl ammonium bromide (HDTMA-Br) surfactant containing Arsenazo III. J Colloid Interface Sci 494:317–324
19. Hasheminejad M, Nezamzadeh-Ejhieh A (2015) A novel citrate selective electrode based on surfactant modified nano-clinoptilolite. Food Chem 172:794–801
20. Nosuhi M, Nezamzadeh-Ejhieh A (2018) An indirect application aspect of zeolite modified electrodes for voltammetric determination of iodate. J Electroanal Chem 810:119–128
21. Kan X, Liu T, Zhou H (2010) Molecular imprinting polymer electrosensor based on gold nanoparticles for theophylline recognition and determination. Microchim Acta 171:423–429
22. Yola M L, Atar N, Eren T, et al. (2015) Correction: Sensitive and selective determination of aqueous triclosan based on gold nanoparticles on polyoxometalate/reduced graphene oxide nanohybrid. Rsc Advances 5:65953–65962
23. Stobiecka M, Deeb J, Hepel M (2009) Molecularly Templated Polymer Matrix Films for Biorecognition Processes: Sensors for Evaluating Oxidative Stress and Redox Buffering Capacity. ECS Trans 19:15–32
24. Zhang J, Wang Y, Lv R (2010) Electrochemical tolazoline sensor based on gold nanoparticles and imprinted poly-aminothiophenol film. Electrochima Acta 55:4039–4044
25. Chao ZG, Yong S, Dong ZQ, et al. (2014) Study on bisphenol A imprinted sensor based on the film of gold nanoparticles. J Funct Mater 45:01099–01103
26. Riskin M, Telvered R, Frasconi M (2010) Stereoselective and chiroselective surface plasmon resonance (SPR) analysis of amino acids by molecularly imprinted Au-nanoparticle composites. Chem Eur J 16:7114–7120
27. Tan F, Zhao Q, Teng F, Sun D, Gao J, Quan X, Chen J (2014) Molecularly imprinted polymer/mesoporous carbon nanoparticles as electrode sensing material for selective detection of ofloxacin. Mater Lett 129:95–97
28. Nosuhi M, Nezamzadeh-Ejhieh A (2018) A sensitive and simple modified zeolitic carbon paste electrode for indirect voltammetric determination of nitrate. Ionics 24:2135–2145
29. Zhao WR, Kang TF, Lu LP, Shen FX, Cheng SY (2017) A novel electrochemical sensor based on gold nanoparticles and molecularly imprinted polymer with binary functional monomers for sensitive detection of bisphenol A. J Electroanal Chem 786:102–111
30. Xue F, Gao ZY, Sun XM (2015) Electrochemical determination of environmental hormone nonylphenol based on composite film modified gold electrode. J Electrochem Soc 162:H338–H344
31. Kiss L, David V, David LG et al (2016) Electropolymerized molecular imprinting on glassy carbon electrode for voltammetric detection of dopamine in biological samples. Talanta 160:489–498
32. Wang F, Zhu LH, Zhang JD (2014) Electrochemical sensor for levofloxacin based on molecularly imprinted polypyrrole–graphene–gold nanoparticles modified electrode. Sensors Actuators B Chem 192:642–647
33. Amani-Beni Z, Nezamzadeh-Ejhieh A (2018) NiO nanoparticles modified carbon paste electrode as a novel sulfasalazine sensor. Anal Chim Acta 1031:47–59
34. Ji Z, Chen W, Wang E (2017) Electropolymerized Molecular Imprinting & Graphene Modified Electrode for Detection of Melamine. Int J Electrochem Sci 12:11942–11954
35. Zhou J, He XW, Li YJ (1999) Binding study on 5,5-diphenylhydantoin imprinted polymer constructed by utilizing an amide functional group1Project 29775011 supported by National Natural Science Foundation of China.1. Anal Chim Acta 394:353–359
36. Wang CL, Hu XL, Ping G (2015) Superparamagnetic Molecularly Imprinting Polymers for Adsorbent and Separation Pentapeptides by Surface ATRP. Sep Sci Technol 50:1768–1775
37. Niknezhadi A, Nezamzadeh-Ejhieh A (2017) A novel and sensitive carbon paste electrode with clinoptilolite nano-particles containing hexadecyltrimethyl ammonium surfactant and dithizone for the voltammetric determination of Sn(II). J Colloid Interface Sci 501: 321–329